

# Controlling the processing of collagen-hydroxyapatite scaffolds for bone tissue engineering

Denys A. Wahl · Eleftherios Sachlos · Chaozong Liu · Jan T. Czernuszka

Received: 19 June 2006 / Accepted: 19 September 2006  
© Springer Science + Business Media, LLC 2007

**Abstract** Scaffolds are an important aspect of the tissue engineering approach to tissue regeneration. This study shows that it is possible to manufacture scaffolds from type I collagen with or without hydroxyapatite (HA) by critical point drying. The mean pore sizes of the scaffolds can be altered from 44 to 135  $\mu\text{m}$  depending on the precise processing conditions. Such pore sizes span the range that is likely to be required for specific cells. The mechanical properties of the scaffolds have been measured and behave as expected of foam structures. The degradation rate of the scaffolds by collagenase is independent of pore size. Dehydrothermal treatment (DHT), a common method of physically crosslinking collagen, was found to denature the collagen at a temperature of 120°C resulting in a decrease in the scaffold's resistance to collagenase. Hybrid scaffold structures have also been manufactured, which have the potential to be used in the generation of multi-tissue interfaces. Microchannels are neatly incorporated via an indirect solid freeform fabrication (SFF) process, which could aid in reducing the different constraints commonly observed with other scaffolds.

## 1 Introduction

A tissue engineering approach has been attempted to regenerate many tissues such as skin, cartilage, bone, liver and heart valves [1]. Tissue engineering requires the use of a temporary porous matrix, called a scaffold, in order to guide the regeneration of the tissue to the desired three-dimensional (3D) shape. In principle, selected cells attach to the scaffold,

migrate into the porous matrix and differentiate to generate new tissue. This can be directly attempted *in vivo* by placing the scaffold in a critical size defect and relying on natural biological signals (i.e. growth factors) to guide the surrounding cells into the scaffold. An alternative would be to recreate the tissue *in vitro* using harvested and cultured cells and mimicking the local defect environment [2].

Bone tissue engineering is aimed at repairing diseased or fractured bone, which cannot be replaced naturally. Skeletal tissue is a highly organised structure comprising mainly type I collagen, nanometre sized carbonate-substituted hydroxyapatite crystals, water and various other non-collagenous proteins. Alike many extracellular matrix proteins, collagen type I presents natural binding sites such as the Arg-Gly-Asp (RGD) and the Asp-Gly-Glu-Ala (DGEA) peptide sequence that modulates the adhesion of osteoblasts and fibroblasts [3, 4]. On the other hand, hydroxyapatite is osteoconductive [5, 6] and a good source of calcium and phosphate ions necessary for the survival of cells. Although collagen and apatite-based products have been widely used individually in biomedical applications, their combination should prove beneficial for bone tissue engineering due to their natural biological resemblance and properties [7, 8].

There are still many uncertainties regarding the optimum requirements for a scaffold in bone tissue engineering. Two of the current discussions are scaffold pore size and porosity; although it is generally agreed that highly porous scaffolds perform better *in vivo* [9]. In general, a scaffold will be successful only if it becomes vascularised and cells within can have access to nutrients and oxygen for their survival [10]. It is believed that such vascularisation—and direct osteogenesis—may happen if the scaffold has large enough interconnected pores of approximately 300  $\mu\text{m}$  in diameter [9, 11]. However, optimal pore sizes are likely to be tissue and cell dependent as it has been observed that for skin tissue engineering

D. A. Wahl (✉) · E. Sachlos · C. Liu · J. T. Czernuszka  
Department of Materials, University of Oxford, Parks Road,  
Oxford, OX1 3PH, UK  
e-mail: denys.wahl@materials.ox.ac.uk

scaffolds required 100  $\mu\text{m}$  pores [12]. Increasing porosity and pore size will inherently compromise the scaffold mechanical properties. A scaffold acts as a temporary support and should be able to withstand forces exerted on it during implantation. Such forces include cellular contraction, fluid flow and local stresses that occur during tissue formation or surgical handling. The importance of mechanical properties is dependent on the purpose of the scaffold, whether needed for a high load- or relatively low load-bearing application. In both cases, some temporary external support (metallic plates and screws) may still be needed during new tissue formation if the scaffolds are not sufficiently stable.

Solid freeform fabrication is a relatively recent technique used in bone tissue engineering. Three dimensional printing technologies have the potential to create scaffolds directly or indirectly (via mould casting) from a computer aided design, with predefined external and internal morphologies. Polyglycolic acid (PGA), polylactic acid (PLLA), polycaprolactone (PCL), hydrogel, hydroxyapatite and collagen are examples of scaffold material that have benefited from SFF technologies [13]. Combined with medical scan data from computerised tomography or magnetic resonance imaging, SFF has been used to generate scaffolds that match the osseous defect very precisely [14, 15]. Furthermore, SFF has achieved for example hydroxyapatite scaffolds with porosity, pore size and shape that optimises the mechanical properties [16] or with a design that facilitates the seeding process and enhances cellular adhesion and proliferation under dynamic conditions [17]. It has also been possible to generate scaffolds directly that mimic multi-tissue interfaces, such as osteochondral tissue. In using different scaffold and cell strategies, hybrid scaffolds have been manufactured that combine an osseous and cartilaginous environment [18].

This paper presents work on the control of the processing of collagen and collagen-hydroxyapatite scaffolds. It will illustrate how the scaffolds can be manufactured to possess specific porosity, mechanical and biodegradation properties and how internal microstructures can be inserted into the scaffold by the use of solid freeform fabrication. The discussion will focus on this ability to tailor biocompatible scaffolds to a particular tissue or defect and in particular the use of hybrid scaffolds to generate multi-tissue interfaces.

## 2 Materials and methods

### 2.1 Scaffold preparation

Fibrillar collagen type I from bovine Achilles tendon (Sigma Aldrich) and hydroxyapatite particles (Capital 60-1, Plasma Biotol) were used to make suspensions of various concentrations. Suspensions of 1, 3 and 5 wt% collagen (1 g of collagen in 100 ml yields a 1 wt% suspension) were prepared by plac-

ing the collagen in an acidic aqueous solution (pH 3.2), the pH being adjusted by drop wise addition of ethanoic acid. The suspensions were then homogenised three times for 1 minute with a conventional blender and the temperature controlled by placing the beaker into an ice bath. De-airing of the suspensions was performed under vacuum at approximately 0.1 kPa for 20 min. The procedure of blending and de-airing was repeated after the addition of hydroxyapatite particles (diameter 15–70  $\mu\text{m}$ ). All collagen suspensions contained 70 wt% hydroxyapatite, in order to mimic the natural composition of skeletal bones. The suspensions were then stored in a refrigerator at 4°C.

The manufacturing of collagen scaffolds [19] and collagen-hydroxyapatite scaffolds [20] has been previously reported. In brief, the aqueous suspensions of collagen-HA were poured into a mould and frozen at either  $-30^{\circ}\text{C}$  or  $-80^{\circ}\text{C}$ . The process of making the moulds will be described in the following section. The samples were then dehydrated hourly in ethanol three times under vigorous stirring to remove the ice crystals and to dissolve the mould material. Three hours of critical point drying using liquid  $\text{CO}_2$  was used to create a dry porous scaffold. In order to create hybrid scaffolds, different collagen suspensions were poured in the moulds and frozen.

Dehydrothermal treatment (DHT), a conventional physical method of crosslinking was applied to the scaffolds by subjecting dry scaffolds to heat dehydration at  $120^{\circ}\text{C}$  under a  $10^{-2}$  mbar vacuum for three days. The temperature was allowed to return to approximately  $20^{\circ}\text{C}$  before removing the vacuum [21].

### 2.2 Solid freeform fabrication (SFF)

A phase change jet printer (T66, SolidScape Inc.) has been used to create moulds of different external shapes and internal structures. Figure 1 shows the indirect process for creating a composite scaffold of pre-designed shape using SFF. The moulds are first designed on computer aided design software (AutoCad 2005, AutoDesk) and printed using biocompatible materials (BioBuild and BioSupport, TEOX Ltd.).

### 2.3 Scaffold characterisation

#### 2.3.1 Microstructural evaluation

Frozen samples were cross-sectioned with a razor blade to approximately one millimetre. The scaffolds were then gold-sputter coated and viewed under a scanning electron microscope (JSM-840F JEOL) operated at 2.5 kV for microstructural evaluation. Image analysis software (ImageJ, Wayne Rasband) was then used to determine the mean pore size and distribution within the scaffold. The porous volume of the scaffolds were calculated using the mass technique and the

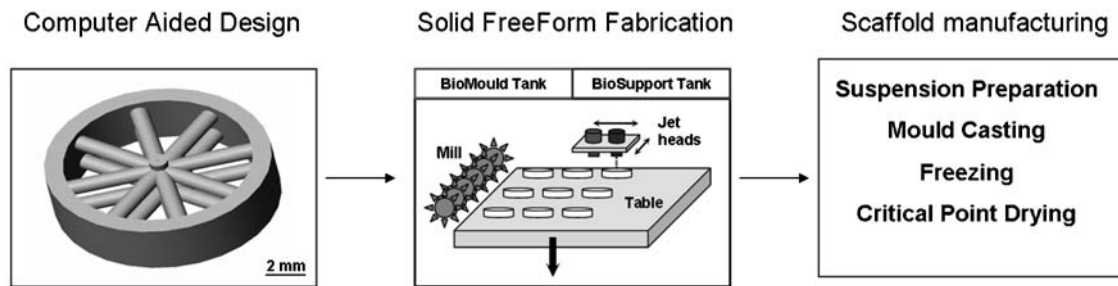


**Fig. 1** The indirect process of scaffold engineering with solid freeform fabrication using a dual phase change jet printer (T66, SolidScape Inc.)

rule of mixtures, knowing the mass of the scaffolds, their linear dimensions (volume), the weight percent ratio of collagen to hydroxyapatite and using the densities of  $1.2 \text{ g/cm}^3$  for collagen and  $3.56 \text{ g/cm}^3$  for hydroxyapatite.

### 2.3.2 Fourier transform infra-red (FTIR)

Infrared spectra were obtained in transmission mode using a FTIR spectrometer (Spectrum 2000, Perkin Elmer) from discs containing critical point dried collagen-HA samples and potassium bromide (KBr) powders. Fifty scans over the range of  $400\text{--}4000 \text{ cm}^{-1}$  were achieved at a resolution of  $2 \text{ cm}^{-1}$  with the background scan subtracted.

### 2.3.3 Differential scanning calorimetry (DSC)

The thermal stability of collagen was measured with DSC (METLER DSC-821e) by placing 5–7 mg of sample in an aluminium pan to which  $15 \mu\text{l}$  of distilled water was added. After a soaking time of 20 min at  $4^\circ\text{C}$ , samples were heated between  $25\text{--}80^\circ\text{C}$  at  $5^\circ\text{C}/\text{min}$  against an empty reference pan. Each scan was repeated three times.

### 2.3.4 Mechanical properties

Scaffolds were subjected to tensile testing at a force rate of  $70 \text{ mN}/\text{min}$  with a Dynamic Mechanical Analyser (DMA7e, Perkin-Elmer) in Hartmann's solution at  $37^\circ\text{C}$ . An average of five runs was used to determine the Young's modulus, which was calculated at the steepest slope of the graph. At low strains, tensile testing is a simple and effective measurement of the Young's modulus of a scaffold.

### 2.3.5 Collagenase degradation

3 wt% collagen-HA scaffolds of 15–20 mg were measured dry and incubated at  $37^\circ\text{C}$  with 1 ml of 0.1 M Tris-HCl (pH 7.4) containing 50 mM  $\text{CaCl}_2$  for  $1/2 \text{ h}$ . A 1 ml of 0.1 M Tris-HCl containing 200 U of bacterial collagenase (Sigma Aldrich) was added to the solution and scaffolds were sub-

jected to 1 Hz in a shaker bath. Samples were taken out at four different time points and placed in ice with an additional 0.2 ml of 0.25M EDTA in order to stop the enzymatic reaction. The samples were then rinsed three times in water and then in ethanol over a period of three hours. The samples were then dried under a flow cabinet for 24 h, remeasured dry and the percentage degradation calculated as the difference between the original and final dry mass. A control scaffold was also measured without the addition of collagenase.

## 3 Results and discussion

### 3.1 Scaffold microstructure

Figure 2 illustrates a cross sectional view of the microstructure of the composite scaffolds at different processing temperatures, showing porosity and walls comprising collagen and hydroxyapatite. The HA particles are mechanically interlocked with the collagen fibrils. The fibrils surround the HA particles to cover fully or partially the particle surface. Collagen fibres bundle together into features that can be described either as dense fibres or sheets, which constitute the frame of the scaffold pores. It can be seen from the images that processing the scaffolds at higher freezing temperatures ( $-30^\circ\text{C}$ ) results in the formation of larger collagen fibres and sheets, of up to approximately 20 and  $500 \mu\text{m}$  in diameter and length respectively, compared to processing at lower freezing temperatures ( $-80^\circ\text{C}$ ) with collagen fibres and sheets of up to approximately 10 and  $150 \mu\text{m}$  in diameter and length respectively. For cell adhesion, it is important to have surfaces with features that are equal or larger than the cell itself. Indeed, a study of non-woven implants containing polyethylene terephthalate fibres of varying diameter ( $2\text{--}40 \mu\text{m}$ ) showed that implants manufactured from smaller fibres decreased the amount of mesenchymal stem cell adhesion [22]. However a more recent study on starch-based scaffolds has found that the combination of nano- and micro-sized fibres increased the morphology, viability and ALP activity of osteoblasts and bone marrow stroma cells [23].

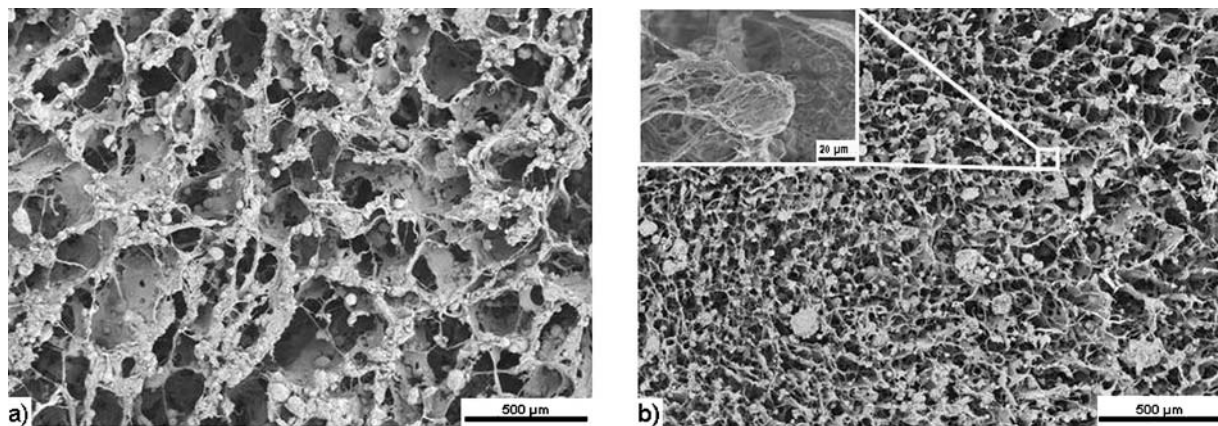


**Fig. 2** Cross-sectional view of the interior of a collagen-HA scaffold with freezing rates of (a)  $-30^{\circ}\text{C}$  and (b)  $-80^{\circ}\text{C}$

From such images, a porosity analysis was applied to measure mean pore size and to plot pore size distribution curves. Figure 3 illustrates the variation of both the collagen content and the freezing rate of the collagen-HA suspensions on the scaffold internal porosity. The composite scaffold with 1 wt% collagen, frozen at  $-30^{\circ}\text{C}$ , resulted in an average pore size of  $135\ \mu\text{m}$  in diameter (assuming spherical pores). This pore size was shown to be sufficient for osteoblastic infiltration in collagen-HA composites [24]. Increasing the collagen content and the freezing rate, at which the ice crystals are formed, also resulted in scaffolds with highly interconnected porosity. However, the pores were now smaller on average and reached a minimum mean of  $44\ \mu\text{m}$  for the 5 wt% collagen-HA scaffold, frozen at  $-80^{\circ}\text{C}$ . The porosities (porous volume percent) of the scaffolds were calculated to be 95% ( $\pm 0.2$ ), 91.9% ( $\pm 0.2$ ) and 87.2% ( $\pm 1.4$ ) for the 1 wt%, 3 wt% and 5 wt% collagen-hydroxyapatite scaffolds respectively. The processing conditions did not affect the porous volume of the scaffolds.

It can be seen from the porosity analysis of Fig. 3 that only the scaffolds of 1 wt% and 3 wt% collagen frozen at  $-30^{\circ}\text{C}$  presented pores over  $300\ \mu\text{m}$  in diameter. It must also be noted that the majority of pores are of  $50\ \mu\text{m}$  or less and are not shown in the graphs. Although pores smaller than  $50\ \mu\text{m}$  may not be sufficient to generate internal vascularisation or sufficient cell penetration needed for the success of an implanted scaffold [9], this limitation can be compensated using solid freeform fabrication. Such technology has the ability to create internal channels of complex geometries within a collagen and collagen-hydroxyapatite scaffold. Using the same concept but without SFF, channels of varying diameters were inserted by the aid of needles into an 85% porous HA scaffold of  $70\ \mu\text{m}$  ( $\pm 4\ \mu\text{m}$ ) interconnecting window size [25]. Human osteosarcoma cell penetration increased with larger channel diameter and was negligible when the cells were seeded on scaffolds without internal channels.

In conclusion, scaffold microstructure may well have an important role in the adhesion and proliferation of cells. However, cell adhesion is also governed by the material itself. Most biodegradable scaffolds require the first step adsorption of soluble proteins to their surfaces. These proteins then uncoil depending on the material to reveal specific binding sites, which allow for different cells to attach. By mimicking the bone tissue material, collagen and collagen-hydroxyapatite scaffolds have the potential to increase osteogenic cell adhesion and proliferation.

### 3.2 Characterisation of the scaffold material

Infrared spectrum of a composite scaffold after critical point drying is presented in Fig. 4. Amide I ( $1640\text{--}1660\ \text{cm}^{-1}$ ) and Amide II ( $1535\text{--}1550\ \text{cm}^{-1}$ ) peaks are characteristic of native collagen type I [26] and the antisymmetric phosphate band ( $1200\text{--}1000\ \text{cm}^{-1}$ ) is characteristic of hydroxyapatite [27]. The carbonate substitution is present to a lesser extent than in natural bone hydroxyapatite. The HA used in the composite scaffold manufacturing process has most probably been sintered at elevated temperatures. Such a process increases the crystallinity of the HA but removes the carbonate substitution of the HA [28]. Stoichiometric HA will resorb slower under acidic environments than substituted HA and therefore will remain for longer periods of time in the body [29].

It is also important that the process does not affect the chemistry of collagen, as cells are shown to attach to a higher degree to surfaces containing natural binding sites [30, 31]. In addition, processing must not alter the tertiary and quaternary structure of collagen, as the inter- and intra-molecular crosslinks that bind the collagen triple-helices together, provide collagen with its relatively high mechanical properties and resistance to biodegradation. Processing was found not have a major effect on the thermal properties of collagen. DSC analysis measured the denaturation temperature

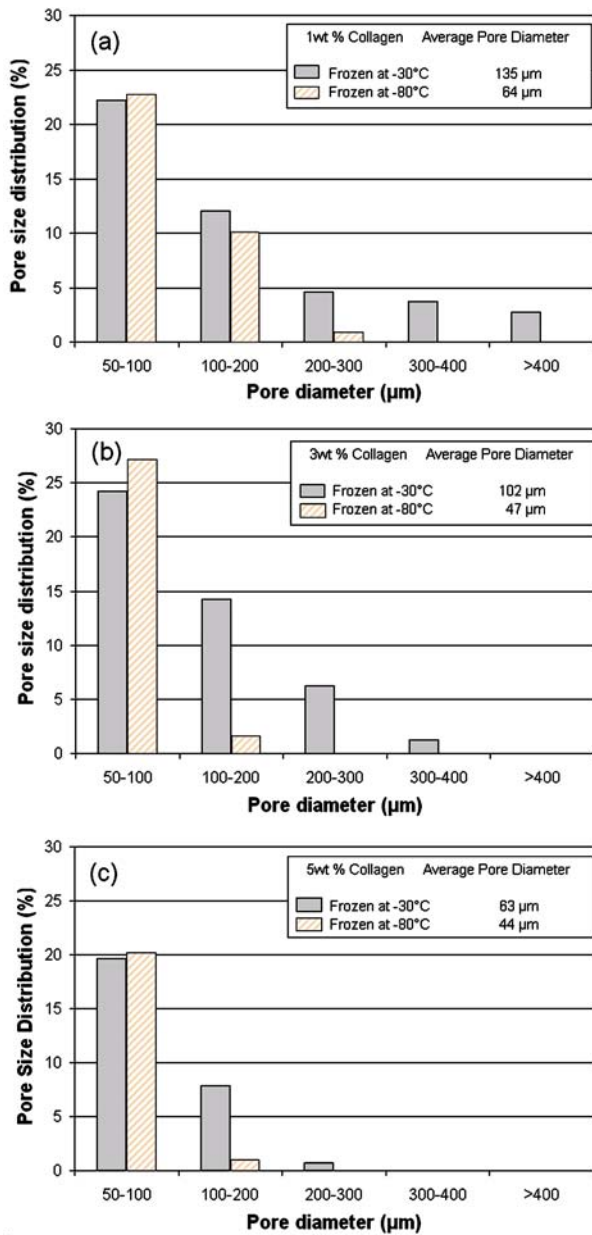


**Fig. 3** Pore size distribution curves of collagen-HA composite scaffolds measured with ImageJ for (a) 1 wt% (b) 3 wt% and (c) 5 wt% collagen, processed at different freezing temperatures

(helix-to-coil transition) at 59.2°C (±0.55) and 58.2°C (±0.6) before and after critical point drying respectively. Due to the intactness of the triple helix of collagen after CPD, the material will be able to withstand the biodegradation of many proteinases such as pepsin and trypsin. It was also shown that the quaternary structure of collagen was not affected by CPD [32].

Scaffolds with interconnected pores have been fabricated from type I collagen and hydroxyapatite particles. The microstructure of the scaffolds is varied by the collagen and hydroxyapatite content and by the freezing temperature of

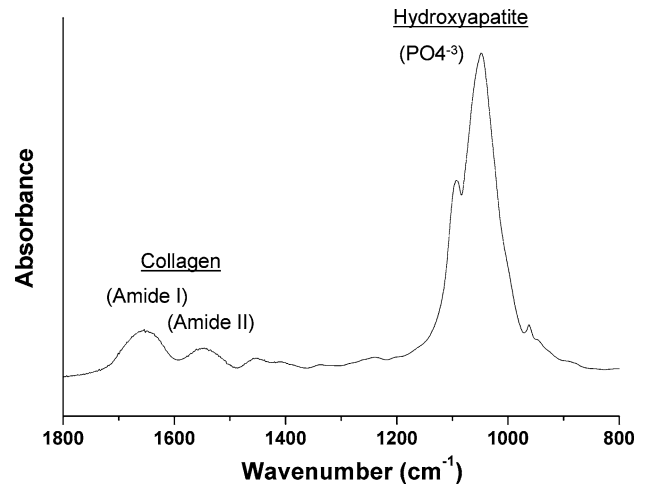


**Fig. 4** FTIR spectra of collagen-hydroxyapatite scaffolds after critical point drying. Typical amide I (1654 cm<sup>-1</sup>) and amide II (1546 cm<sup>-1</sup>) peaks, as well as the phosphate stretching (1048.5 cm<sup>-1</sup>) peak; indicate the presence of both collagen Type I and hydroxyapatite respectively

the manufacturing process. The influence of the processing conditions on the mechanical and biodegradation properties of the scaffolds will now be investigated.

### 3.3 Mechanical and biodegradation properties of collagen-HA scaffolds

#### 3.3.1 Mechanical properties

The effect of collagen content on the wet mechanical properties will be considered first. Table 1(a) shows the advantage of increasing the collagen and hydroxyapatite content of the initial suspension on the mechanical properties of the scaffolds. Although there is no distinct proportionality between collagen content and Young’s modulus, an increase in the Young’s modulus of the scaffold can still be observed as the porous volume of the scaffold decreases (denser scaffold). Scaffolds behave like foam structures where the mechanical properties are dependent on the properties of the scaffold material and on their relative densities (the density of the foam divided by that of the solid) [33]. Assuming that the densities of collagen and hydroxyapatite are similar in all scaffolds, their Young’s moduli are directly proportional (to the power ‘n’ depending on the unit pore structure) to the scaffold density. Therefore increasing the collagen and hydroxyapatite content of the starting suspension renders a denser scaffold and an increase in stiffness. This phenomenon has been demonstrated in other scaffold materials used for bone tissue engineering [9].

The second investigation was to analyse the effect of freezing rate and DHT crosslinking method on the wet mechanical properties of composite scaffolds. The results show that

**Table 1** The wet mechanical properties of collagen-HA scaffolds

Mean  $\pm$  S.D.  $n = 5$ ; for Young's modulus values only, significantly different ( $p < 0.05$ ) between 1 wt% and 5 wt% and ( $p < 0.01$ ) between 3 wt% and 5 wt%, by Student  $t$ -test  
 Mean  $\pm$  S.D.  $n = 5$ , all significantly different ( $p < 0.01$ ) by Student  $t$ -test

(a) The effect of collagen and hydroxyapatite content in composite scaffolds			
Collagen	1 wt%	3 wt%	5 wt%
Young's modulus (kPa)	37.3 $\pm$ 29.7	40.8 $\pm$ 8.2	75 $\pm$ 14.1
Porous volume (%)	95 $\pm$ 0.2	91.9 $\pm$ 0.2	87.2 $\pm$ 1.4

(b) The effect of processing conditions on 3 wt% collagen-HA scaffolds			
	Processed at $-30^{\circ}\text{C}$	Processed at $-80^{\circ}\text{C}$	Processed at $-30^{\circ}\text{C}$ + DHT
Young's modulus (kPa)	40.8 $\pm$ 8.2	23 $\pm$ 3.6	82.2 $\pm$ 23.4

processing at lower freezing temperatures decreased the Young's modulus of the scaffold. The thinning of the pore fibres and sheets measured from Fig. 2 could explain for the lower modulus measured for the two composites of similar porosity (3 wt%). Indeed, it is known that as the ice crystals grow in multiple directions in the collagen/ethanoic acid suspension, the collagen fibrils are pushed to the interstices of the ice crystal network [34]. With slower rates of ice crystal formation (higher freezing temperature), more collagen is pushed in between the interstices and thicker walls are created. These denser features consist of an extensive array of packed collagen fibres, which interlock mechanically, resisting strain upon a given stress and give rise to an overall higher Young's modulus.

As expected, dehydrothermal treatment increased the Young's modulus of the composite scaffolds. Such heat treatment under vacuum was first attempted to insolubilise gelatine [35] and then to improve the stability and mechanical properties of collagen [21]. Severe dehydration under vacuum is believed to induce intermolecular crosslinks via amide formation and is an established method for physically crosslinking collagen. It can be noted that only a few biodegradable porous implants present mechanical properties as high as bone and as the implants degrade, their mechanical properties will inherently decrease. The mechanical properties of the composite scaffolds presented here are of values similar to crosslinked bovine collagen scaffolds measured under wet tensile conditions [36] but are much lower than cortical and cancellous bone, which range between 7–30 GPa and 0.05–0.5 GPa respectively [37]. Chemical crosslinking may be necessary in many cases to induce higher amounts of crosslinks and stiffer scaffolds. However, chemical ways of crosslinking implants have had drawbacks of toxic residual waste products, which may lead to undesired cellular responses [38]. For a load-bearing application, if the mechanical properties of the scaffolds are insufficient, metallic plates and screws may be required for stability until the tissue has regenerated enough to withstand the local stresses.

### 3.3.2 Biodegradation properties

Another important factor for scaffolds when designing temporary or long-term implants for tissue engineering is their biodegradability. In order to mimic partially the *in vivo* conditions of biodegradation, samples were placed in a collagenase environment at body temperature and at a mechanical stimulus of 1 Hz. All samples degraded (loss in weight) except for the control scaffolds where collagenase was not present in solution. The degradation rates of collagen-HA scaffolds are represented in Fig. 5. Scaffolds of different pore size distribution, achieved by varying the freezing temperature, had similar degradation rates when exposed to collagenase (13.5 and 16.4%/h respectively). However, a marked difference occurred after dehydrothermal treatment of the scaffolds (31.9%/h). These values are subject to the concentration of the collagenase solution and are not likely to be identical to *in vivo* conditions.

Collagenase (Type I) is an enzyme released by osteoclasts in order to breakdown the collagenous network in bones. It cleaves preferentially at the Y-Gly bond in the amino sequence -Pro-Y-Gly-Pro- and is capable of breaking more than 100 peptide bonds on each  $\alpha$ -chain of the tropocollagen helix [39]. *In vivo*, collagen-based implants will be subjected

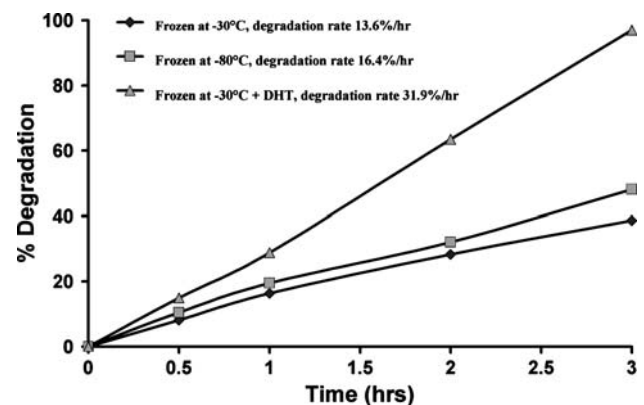


**Fig. 5** Collagenase degradation rates of 3 wt% collagen-hydroxyapatite scaffolds processed at  $-30^{\circ}\text{C}$ ,  $-80^{\circ}\text{C}$  and after dehydrothermal treatment at  $120^{\circ}\text{C}$  for three days

to the enzymatic biodegradation from collagenases found in the extra-cellular matrix of bones. Many reports have demonstrated the ability of dehydrothermal treatment to lower the degradation rate of collagen scaffolds, because of its ability to form intermolecular crosslinks [21, 39]. However, 3 days of dehydration at 120°C under vacuum had the opposite effect and resulted in an increase in the degradation rate *in vitro*. This is potentially the result of collagen partial denaturation due to oxidative reactions at elevated temperatures, highlighted by other authors when processing at temperatures above 110°C [40–42]. DSC measurements of critical point dried scaffolds measured the denaturation temperature to be 58.2°C ( $\pm 0.6$ ) and 46.5°C ( $\pm 1.2$ ) before and after severe dehydration respectively. The lowering of the denaturing temperature due to DHT to values close of gelatine [43] confirms the disorganisation of the collagen structure. If the physical crosslinking method using dehydrothermal treatment avoids the potential risk in retaining toxic molecules that arise from chemical crosslinking, caution must be taken, as elevated temperatures of dehydration will cause irreversible denaturation of the collagen molecule [44].

As well as controlling the microstructure, mechanical and biodegradation properties of biocompatible scaffolds, further engineering may be necessary for the success of the future implant. Scaffolds must permit for sufficient vascularisation to take place for cells to survive and in some application, such as osteochondral tissue engineering, scaffolds may be required to be hybrid structures.

### 3.4 Further engineering the collagen-hydroxyapatite scaffolds

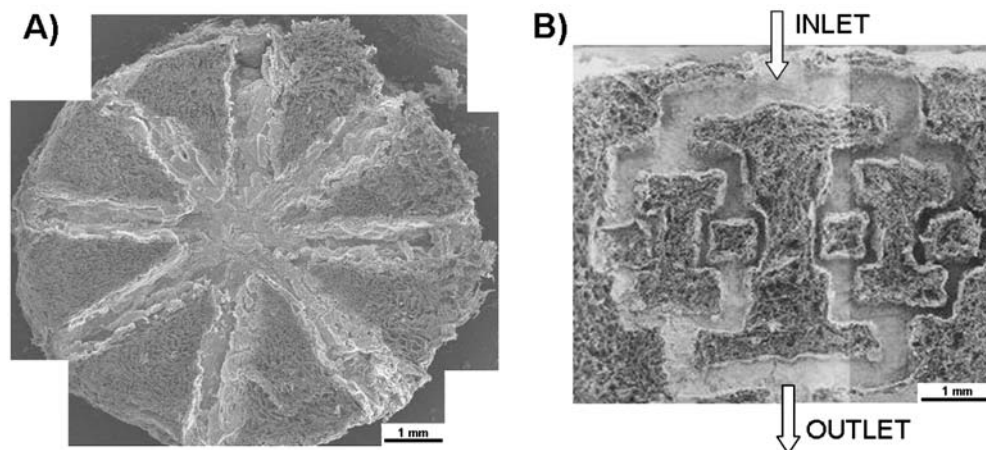
#### 3.4.1 The incorporation of internal microchannels

Figure 6 shows the ability to create collagen and collagen-hydroxyapatite scaffolds from indirect SFF. In the

manufacturing process (Fig. 1), the printing and mould material, BioSupport and BioBuild, are water and ethanol soluble respectively. Their dissolution can therefore easily be incorporated in the scaffold production. Internal channels have been built-in with various designs and have been manufactured as small as 135  $\mu\text{m}$  in diameter.

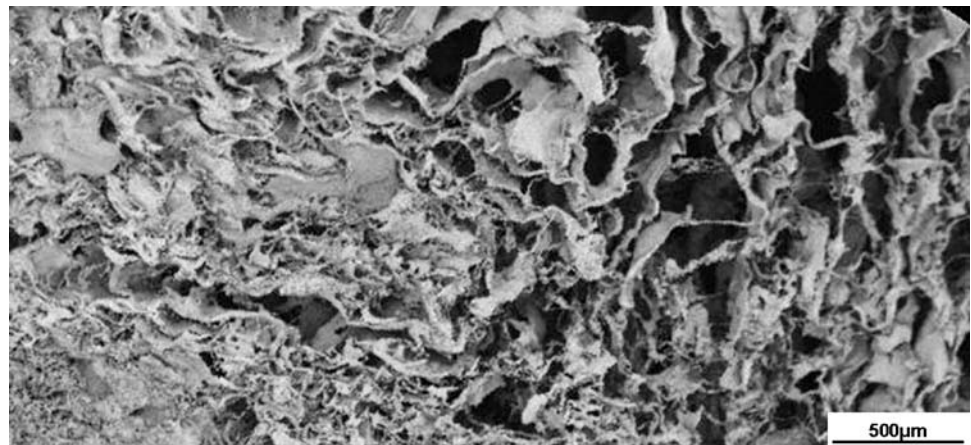
It is important to understand the requirements for generating new tissues. Unlike cartilage, which is very slow to heal itself naturally, bone is able to regenerate fully, until a certain critical defect size, due to a large network of vascularisation. Cells require oxygen and nutrients in order to survive and therefore bone cells are found no further than 300  $\mu\text{m}$  away from a blood vessel [45]. One of the major problems during *in vitro* seeding of cells on a scaffold is the diffusion barrier constraint that causes cellular entrapment, asphyxiation and necrosis [13]. Figure 6(a) shows a design of a collagen-hydroxyapatite scaffold aimed at creating pathways for internal vascularisation. This may be of importance when using denser scaffolds with pore sizes unfavourable to vascularisation ( $< 300 \mu\text{m}$ ), but where good mechanical properties are required. Another advantage of being able to insert internal channels in a scaffold is in order to pump fluids from one single inlet to one single outlet, depicted in Fig. 6(b) using a collagen scaffold. By having fluid pumping within the scaffold, the cells would be in close contact with nutrients for their survival, which may lead to a better growth of three dimensional tissues *in vitro*.

In engineering new tissue, it is crucial for the scaffold to possess many chemical and structural properties, of which aesthetics may not have a significant role to the success of the implant. But for the patient, who requires for example a facial or cranial replacement, it is necessary to obtain the right shape of the implant in order to avoid patient discomfort (more noticeably disfigurement) and to increase the chances of direct union between the implant and the surrounding tissue. Many such repairs are currently achieved by grafting



**Fig. 6** Collagen-hydroxyapatite (a) and collagen scaffold (b) with various internal microchannel designs. Minimum diameter of channel is measured at 135  $\mu\text{m}$

**Fig. 7** Pore size gradient across a scaffold made from a 5 wt% collagen suspension (left) and a 1 wt% collagen suspension (right), both frozen at  $-30^{\circ}\text{C}$ . The pore size distribution curves of the scaffolds are outlined in Fig. 3



autologous bone from the iliac crest, whole or parts of ribs, sternum, and scapula or from the skull itself. In most cases, the procedure requires two operations and the graft may require some manual modelling or the joining of fragments by fibrin glue to fit precisely the osseous defect [46]. Limitations of autografts also include pain and morbidity at the donor site and a shortage of available material [47]. A current trend in tissue engineering is therefore to tailor the scaffold to the precise size and shape of the defect requiring treatment. From patients medical scan data, extrapolated computer aided designs can be linked to solid freeform fabrication processes and the designs printed three-dimensionally to the appropriate defect dimensions. Direct and indirect SFF allows printed scaffolds or moulds to have a controlled external shape and to incorporate internal structures within [13, 14, 19].

### 3.4.2 The creation of a gradient pore size

We have shown that we can tailor the porous properties of a scaffold by adjusting the collagen content and the freezing rate of the collagen and collagen-hydroxyapatite suspension. A gradient pore structure has been created within a scaffold to further optimise this processing. Figure 7 shows a hybrid structure of a collagen scaffold, made from a 1 wt% collagen suspension and a 5 wt% collagen suspension. Such single but heterogenous scaffolds may have the potential to facilitate the growth of different tissues within a scaffold. Indeed, it was earlier described that different cells may have a preference for different pore sizes and optimising these for the right application is necessary.

Single heterogenous scaffolds have the slight advantage of not requiring sutures or fibrin glue to bind different scaffolds together. For example, a PGA mesh has been sutured to a collagen-hydroxyapatite scaffold and seeded with chondrogenic and osteogenic cells respectively [48]. For multi-tissue engineering, cell seeding strategies vary between one single cell source seeded on one part of the scaffold, two different cell sources seeded on the scaffold, one single cell source

having multi-tissue differentiation capacities and finally a cell-free strategy, which relies on transforming growth factors and local cells [18]. The use of collagen and collagen-HA hybrid scaffolds in osteochondral tissue engineering has still not been fully investigated and may prove beneficial in the regeneration of multi-tissue interfaces.

## 4 Conclusion

Collagen and collagen-hydroxyapatite scaffolds for bone tissue engineering have been created using a solid freeform technology and critical point drying. Tailoring the processing conditions has achieved a control over the microstructure, biodegradation and mechanical properties of the scaffolds. Caution is to be taken when crosslinking collagen at  $120^{\circ}\text{C}$  using the conventional dehydrothermal treatment because of the resultant denaturation of the collagen triple helix, which leads to a faster degradation rate after exposure to collagenase. Hybrid scaffolds for multi-tissue engineering have been created and internal microstructures inserted using a dual phase change (3D) printer. Controlling the processing of biocompatible collagen-based scaffolds may lead to a better understanding of the cellular requirements necessary for successfully regenerating new bone.

**Acknowledgments** The authors would like to thank the support of EPSRC for the doctoral training award, the Wellcome Trust Grant 074486 and to Prof. C. Grovenor for the provision of the laboratory facilities.

## References

1. R. CORTESINI, *Transpl. Immunol.* **15** (2005) 81.
2. F. R. ROSE and R. O. C. OREFFO, *Biochem. Biophys. Res. Commun.* **292** (2002) 1.
3. S. DEDHAR et al., *J. Cell Biol.* **104** (1987) 585.
4. W. D. STAATZ et al., *J. Biol. Chem.* **266** (1991) 7363.
5. G. T. CRAIG et al., *Biomaterials* **10** (1989) 133.
6. E. LANDI et al., *J. Eur. Ceram. Soc.* **23** (2003) 2931.
7. A. L. BOSKEY, *Calcif. Tissue Int.* **63** (1998) 179.



8. D. A. WAHL and J. CZERNUSZKA, *Eur. Cell. Mater. J.* **11** (2006) 43.
9. V. KARAGEORGIU and D. KAPLAN, *Biomaterials* **26** (2005) 5474.
10. M. NOMI et al., *Mol. Aspects Med.* **23** (2002) 463.
11. E. TSURUGA et al., *J. Biochem.* **121** (1997) 317.
12. F. J. O'BRIEN et al., *Biomaterials* **26** (2005) 433.
13. E. SACHLOS and J. CZERNUSZKA, *Eur. Cell. Mater. J.* **5** (2003) 29.
14. M. LEE et al., *Biomaterials* **26** (2005) 4281.
15. H. S. TUAN and D. W. HUTMACHER, *Comput. Aided Des.* **37** (2005) 1151.
16. S. J. HOLLISTER et al., *Biomaterials* **23** (2002) 4095.
17. B. LEUKERS et al., *J. Mater. Sci. Mater. Med.* **16** (2005) 1121.
18. I. MARTIN et al., *J. Biomech.* In Press (2006).
19. E. SACHLOS et al., *Biomaterials* **24** (2003) 1487.
20. E. SACHLOS et al., *Mater. Res. Soc. Symp. Proc.* **758** (2003) 187.
21. K. WEADOCK et al., *Biomater. Med. Devices Artif. Organs* **11** (1983) 293.
22. Y. TAKAHASHI and Y. TABATA, *J. Biomater. Sci. Polym. Ed.* **15** (2004) 41.
23. K. TUZLAKOGLU et al., *J. Mater. Sci. Mater. Med.* **16** (2005) 1099.
24. M. ITOH et al., *Biomaterials* **25** (2004) 2577.
25. F. R. ROSE et al., *Biomaterials* **25** (2004) 5507.
26. I. V. YANNAS, *J. Macromol. Sci. Rev. Macromol. Chem. Phys.* **C 7** (1972) 49.
27. I. REHMAN and W. BONFIELD, *J. Mater. Sci. Mater. Med.* **8** (1997) 1.
28. G. C. KOUMOULIDIS et al., *J. Coll. Interf. Sci.* **259** (2003) 254.
29. A. KOCIALKOWSKI et al., *Injury* **21** (1990) 142.
30. B. D. BOYAN et al., *Biomaterials* **17** (1996) 137.
31. U. MEYER et al., *Eur. Cell. Mater. J.* **9** (2005) 39.
32. E. SACHLOS, *D Phil thesis, Oxford University* (2004) 77.
33. M. F. ASHBY and D. R. H. JONES, in "Engineering Materials 2: An Introduction to Microstructures, Processing and Design" (Pergamon Press, 1986) p. 250.
34. H. SCHOOF et al., *J. Crystal Growth* **209** (2000) 122.
35. I. V. YANNAS and A. V. TOBOLSKY, *Nature* **215** (1967) 509.
36. P. ANGELE et al., *Biomaterials* **25** (2004) 2831.
37. W. BONFIELD, et al., *Acta Materialia* **46** (1998) 2509.
38. W. E. HENNINK and C. F. VAN NOSTRUM, *Adv. Drug. Deliv. Rev.* **54** (2002) 13.
39. K. S. WEADOCK et al., *J. Biomed. Mater. Res.* **32** (1996) 221.
40. M. GEIGER, *PhD thesis, Friedrich-Alexander-Universität Erlangen* (2001) 84.
41. S. D. GORHAM, et al., *Int. J. Biol. Macromol.* **14** (1992) 129.
42. M.-C. WANG, et al., *Biomaterials* **15** (1994) 507.
43. A. BIGI et al., *Biomaterials* **25** (2004) 5675.
44. T. J. WESS and J. P. ORGEL, *Thermochimica Acta* **365** (2000) 119.
45. P. J. KELLY, *J. Bone Joint Surg. Am.* **50** (1968) 766.
46. M. ARTICO et al., *Surg. Neurol.* **60** (2003) 71.
47. R. R. BETZ, *Orthopedics* **25** (2002) S561.
48. D. SCHAEFER et al., *Arthritis Rheum.* **46** (2002) 2524.